2d Tomographic Reconstruction of Trace Gas Distributions from Long-path DOAS Measurements: General Approach, Validation and Outlook on an Experiment on an Urban Site

A. Hartl *, K.U. Mettenorf, B.C. Song, U. Platt, I. Pundt

Institute of Environmental Physics, University of Heidelberg, Heidelberg, Germany

Abstract – DOAS-tomography is a remote sensing technique to retrieve 2 or 3 dimensional distributions of atmospheric trace gas concentrations. It combines Differential Optical Absorption Spectroscopy yielding average concentrations of trace gases along long light paths with reconstruction methods from computerised tomography. Here we refer to reconstructions from ground based measurements using artificial light sources. We present our reconstruction method, consisting in a discrete approach, and show that for locally confined distributions like dispersions plumes, reconstruction quality and reconstructed total concentrations can be tremendously improved by choosing an optimal parametrisation in terms of basis functions and dimension of the discretisation grid. Choice of the light path geometry has large influence as well, where for constant number of light paths, increasing the number of emitting systems tends to improve reconstructions. The method is applied to data from an indoor measurement and results are in good agreement with expectations, while the impact of measurement errors is moderate. This method will be applied to an experiment intended to measure cross sections of trace gas distributions over the city centre of Heidelberg, Germany, taking place in spring and summer 2005.

Keywords: Trace Gas Distributions, DOAS, Tomography, Gaussian Dispersion Plumes.

1. INTRODUCTION

Knowing the exact amount and distribution of trace gases in the atmosphere on microscales is important for assessing air quality in polluted areas, identifying and estimating local emissions and evaluating chemical transport models. Spatial concentration fields can be obtained by a sufficient number of point measurements, but possibly only at large instrumental expense and with high sensitivity to spatial and temporal fluctuations. Alternatively, remote sensing methods like the Differential Optical Absorption Spectroscopy (DOAS) (e.g. Platt, 1994) provide mean concentrations along light paths -in the case of DOAS for species such as NO_2, O_3, SO_2, HCHO, HONO, BrO and aromatics. Here, we consider ground based measurements with an artificial light source and reflectors that, after a distance of several hundred meters up to a couple of kilometers, redirect the light back into the emitting system where it is analysed (so called Long-Path (LP) DOAS). Using measurements along several light paths, information on the spatial distribution can be obtained by various retrieval techniques. We examine a discrete tomographic approach that was used in (Laepple et al., 2004) for the reconstruction of a cross section through a NO_2 motorway emission plume perpendicular to it from measurements by two telescopes and 16 light paths in total (see (Pundt et al., 2005) for experimental details). The unknown concentration field is parametrised by a limited number of local –box or linear– 'basis' functions and the resulting discrete concentration values are fit to the data by a least squares principle. It is well known that for narrow peaks, in our case Gaussians emerging from the semi-empirical approach which describes the turbulent and advective dispersion of pollutants in the atmosphere by a Gaussian diffusion equation, discretisations can be chosen that lead to highly under-determined systems, if additional constraints are chosen. The solution with smallest norm of the concentration vector is examined in detail with respect to parametrisation and peak extension. Different geometries with 36 light paths –a realistic number for LP-DOAS measurements– are compared. Furthermore, a 'grid translation' method proposed in (Verkruysse and Todd, 2004) for the case of box basis functions is modified for the linear case. The simulation results are used for an indoor experiment, where one or two cylinders filled with NO_2 were placed into an area that was monitored by three telescopes and 39 light paths in total (Mettendorf et al., in preparation). A similar, yet less regular, geometric setup with at least 16 light paths will be used to measure 2d trace gas distributions over the city of Heidelberg.

First considerations for tomographic measurements for atmospheric gas concentrations by laser scanning can be found in (Wolfe and Byer, 1982) but the experimental proposal has not been carried out and their analytic reconstruction method, adopted from medical systems, is not applicable in our case. On the other hand, a variety of studies was dedicated to the remote sensing of indoor gas concentrations and their dispersion by different experimental techniques (e.g. Yost et al., 1994; Drescher et al., 1997; Fischer et al., 2001). Theoretical studies in this field dealing with the performance of algorithms usually use a discrete box approach and least squares solutions minimising some quadratic functional of the concentration vector (Todd and Ramachandran, 1994; Price et al., 2001) or maximising logarithmic measures of likelihood or expectation (Samanta and Todd, 2000). A method suggested in (Drescher et al., 1996) constists in fitting a certain number of Gaussians with variable variances, maxima and positions to data from chamber dispersion experimemts. Todd and Bhattacharyya (1997) examine indoor measurement setups with one to four emitting systems and fan beam configurations (90°-360°), but for a very large number of rays (at least 120) and including mirrors to generate projection-like light paths. Neither of the studies mentioned has been systematic with respect to the shape or extension of the concentration distributions or the effects of different parametrisations, but all authors stress the fact that results may depend very much on the specific distributions considered.

2. METHOD

* Corresponding author: andreas.hartl@iup.uni-heidelberg.de

2.1 Discretisation and Least Squares Minimum Norm Solution

Tomographic DOAS measurements provide integrated concentrations $d_i = \int_i ds\, c(\mathbf{r})$ along a number of light paths i. The unknown concentration field is parametrised by a limited number of local 'basis' functions $c(\mathbf{r}) \cong \sum_j x_j b_j(\mathbf{r})$, where for box functions x_j represent concentration values within the boxes of the discretisation grid, while for linear functions x_j are concentration values on the grid nodes and values in between are linearly interpolated (see (Laepple et al., 2004) for details). The resulting discrete, linear system $(Ax)_i = d_i$ is replaced by a least squares principle. The matrix A contains all information about discretisation and light path geometry. As mentioned, for peak distributions usually the under-determined case applies, and we choose the solution minimising the norm of the vector x_j. Iterative algorithms converging to this kind of solution have widely been studied in image reconstruction; we use the Simultaneous Iterative Reconstruction Technique (SIRT), a simple scheme that proved robust to measurement errors. Additionally a constraint for positive concentration values is implemented (c.f. (Laepple et al., 2004) and references therein).

2.2 Reconstruction Quality

The evaluation of a reconstruction depends on what features one is mostly interested in, e.g. to get the correct maximum concentrations of toxic pollutants is important if human health is concerned. In image reconstruction the overall quadratic misfit between the test and reconstructed distribution is commonly taken as a quality criterion. It is known as nearness, if normalised to give 1 if the reconstructed field is just the spatial mean of the test distribution:

$$nearness = \frac{1}{N}\left(\int dA \left(c(\mathbf{r}) - \sum_j x_j b_j(\mathbf{r})\right)^2\right)^{\frac{1}{2}} \qquad (1)$$

with $N = \left(\int dA \left(c(\mathbf{r}) - \bar{c}(\mathbf{r})\right)^2\right)^{\frac{1}{2}}$ and all integrals referring to the reconstruction area. For narrow peaks, reconstruction of the precise shape of the distribution might not be feasible, so, thinking of emission plumes, the precision of amounts of concentration reconstructed within the peaks is also considered in the following.

2.3 Grid Translation

For coarse, irregular light paths, the choice of a single (regular) discretisation grid is to some extent arbitrary and for peak distributions by no means likely to be the ideal one. This led Verkruysse and Todd (2004) to take into account reconstructions from several grids, shifted against each other in either or both directions in the plane. We modify their method for the linear discretisation by taking the average of the individual reconstructions.

3. SIMULATION RESULTS FOR GAUSSIAN PEAKS

To study the reconstruction of Gaussians, we use the measurement configuration of Fig. 1 with three telescopes in the corners of a square area of 100×100 *arbitrary units* and 36 light paths in total. The Gaussian test distributions are located randomly in the area and variances vary in four ensembles from σ =3 *a.u.* to 30 *a.u.* Taking the extension of the distribution as 2×3×σ (at 3σ the maximum value has fallen to 1%), ensemble 1, containing narrow peaks, represents the lower limit of distributions detectable by this coverage with light paths, whereas large peaks from ensemble 4 smoothly extend over the whole area.

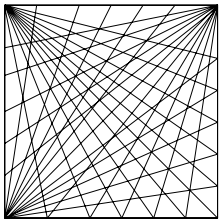

Figure 1. Light path setup with three telescopes, each emitting 12 beams in a 90°-fan. Every beam is reflected back into the telescope by a retro-reflector.

Fig. 2 shows total reconstruction errors (i.e. nearness, Fig. 2a) and deviations of total amounts of concentration within the reconstructed peak relative to the original one (Fig. 2b) versus the dimension of the reconstruction grid for the bilinear parametrisation. Ensemble means are shown for one peak and four peaks (concentration maxima between 0.1–1 *a.u.*) and 300 random samples in each ensemble.

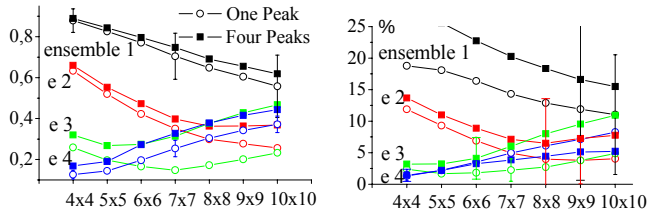

a) Nearness

b) Relative deviation of integrated peak concentration

Fig. 2 Ensemble mean nearness (a) and absolute values of the relative difference between reconstructed and original amounts of concentration within the peak (b) for linear parametrisation (for $n \times n$ pixels the dimension of the bilinear grid is $(n+1)\times(n+1)$). Extensions of the peaks increase from ensemble 1 to 4.

For narrow peaks, the overall reconstruction error can be drastically reduced by choosing high dimensional grids. The systems of equations are under-determined by a factor up to 3, where the additional constraints come from the iteration start serving as a priori and the positivity constraint for the concentration values. Dividing the reconstruction error into one part that is due to imperfect representation of the real concentration field by the basis functions (discretisation error) and another one which is the misfit between the best possible representation and the actual inversion result (inversion error), it can be shown (Hartl et al., in preparation) that for increasing grid dimension the inversion error part increases and the decreasing total reconstruction error is solely a discretisation effect. Comparing box and bilinear discretisation, it furthermore can be shown that not only is the discretisation error smaller for the linear discretisation, but also the inversion error -at least for the reconstruction principle and test distributions considered here. The same trend as for nearness exists for the error of amounts of con-

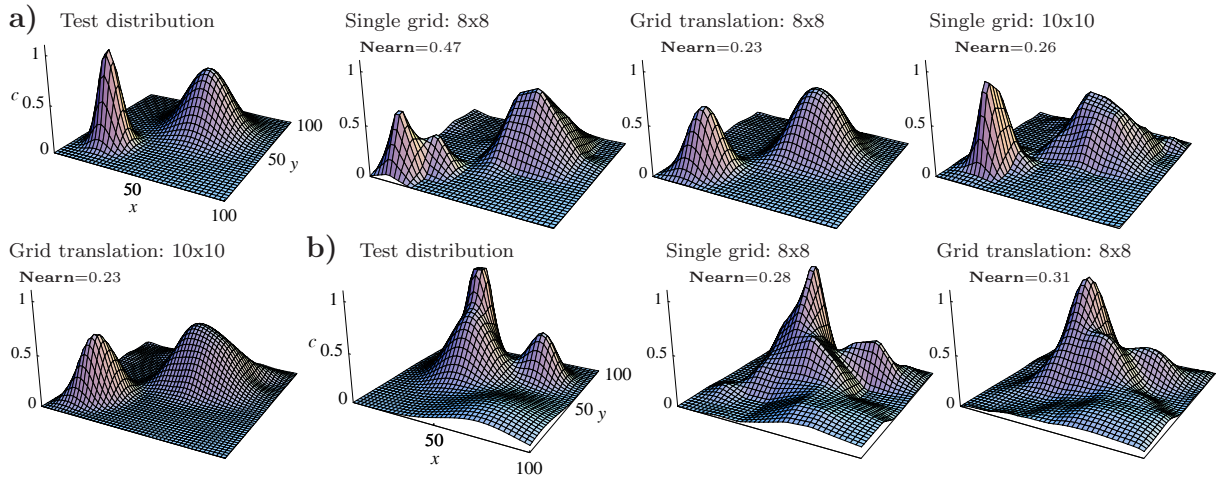

Figure 3. Reconstruction of two (a) and four (b) peaks for bilinear parametrisation using a single, regular grid and an averaging grid translation scheme, respectively. The original grid is shifted four times in each direction.

centration reconstructed within the peak. This is not an effect of discretisation as the pixel length is taken into account in the extension of the reconstructed plume (Hartl et al., in preparation). Deviations refer to ensemble means and averages over random peak locations, but still the numbers (around 20% for one narrow peak and around 30% for four narrow peaks; less than 5(10)% for large plume(s)) can be taken as rough estimates for the precision of reconstructed total concentrations.

Fig. 3 shows examples for the reconstruction of two (Fig. 3a) and four (Fig. 3b) peaks, respectively, comparing reconstructions from a single grid and from averaging over translated grids. The grid was shifted four times in each direction and clearly this reduces accidental features due to the choice of a single grid. In general, the nearness is reduced by applying the averaging scheme, while concentration integrals remain largely unaltered and the peak maximum values decrease (Hartl et al. in preparation).

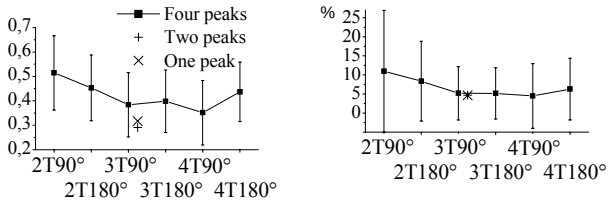

a) Nearness versus geometry. b) Rel. deviation of integrated peak concentration vs geometry.

Figure 4. Ensemble mean values for four peaks from ensembles 1 to 3 and geometries as described in the text. a) Nearness. b) Absolute values of the relative difference between reconstructed and original amounts of concentration within the peak. For geometry 3T90° values for one and two peaks are also shown. Reconstruction on an 8×8 bilinear grid without grid translation.

Finally, Fig. 4 shows nearness and total peak concentrations for different geometries, each of them generated by 36 light paths. They consist of two to four telescopes sitting either in the corners (90°-beam fans) or in the baseline centers (180°-beam fans) of the square (the geometry of Fig. 1 is denoted 3T90° here). Variances of the test distributions vary within the first three ensembles, but the order of the geometries does not depend very much on the choice of the distributions. Clearly, there are distinct differences between the geometries, where increasing the number of telescopes improves reconstruction quality, except for the 180°-fan geometries. Here the coverage with light paths becomes more irregular and sparse when keeping the number of light paths constant (in contrast to the procedure in (Todd and Bhattacharyya, 1997)). The influence of measurement errors on different geometries is studied elsewhere (Hartl et al., in preparation).

4. APPLICATION TO AN INDOOR EXPERIMENT

A light path setup similar to the one shown in Fig. 1, on an area of 15×10 m^2 and with 39 instead of 36 light paths for instrumental reasons, was realised in an indoor experiment, mainly to study the performance of a new instrument (Mettendorf et al., in preparation). This instrument emits up to six rays all at once instead of just one as the conventional ones. In the experiment, four beams were emitted by each of the three telescopes and four

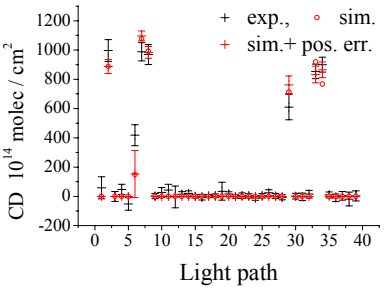

Figure 5. Example for measured and modeled column densities for one cylinder. The light path length is twice the geometrical one. Errors in the simulation refer to the uncertainty in the cylinder position.

scans were necessary to complete the whole geometry of 39 light paths. One or two cylinders of 2m diameter filled with NO_2 were used to simulate locally confined concentration distributions at

different positions of the test area. Fig. 5 shows concentration integrals (so called column densities) along the 39 light paths for one cylinder, on the one hand from simulations and on the other from experiment, for one of the positions. They agree reasonably well within all uncertainties. Fig. 6 shows profiles in one direction through the concentration distribution reconstructed from the data of Fig. 5 and how it compares with theoretical ones. Fig. 6a illustrates how the reconstruction from ideal model data on the regular 12×12 bilinear grid differs from the best possible representation of the cylinder distribution on this grid (referred to as inversion error above). Also shown the peak reduction resulting from the averaging grid translation scheme. Finally, Fig. 6b shows the sensitivity of the reconstruction to the measurement errors from Fig. 5. Relative errors on the data and the concentration values are of the same order.

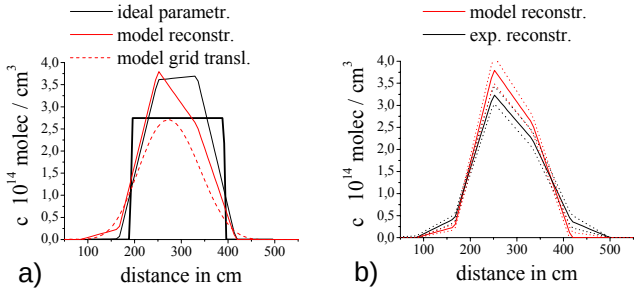

Figure 6. Profiles for the cylinder position as in Fig. 5. a) Model reconstruction refers to reconstruction from simulated data. Grid translated five times in each direction. b) Dotted lines refer to 1σ-errors as in Fig. 5. All reconstructions on a 12×12 bilinear grid.

5. CONCLUSION AND OUTLOOK

Facing a modest number of light paths, the possibility of reconstructing atmospheric trace gases from tomographic LP-DOAS measurements crucially depends on the shape, extension and spatial variability of the distributions compared to the mesh size formed by the light paths. In contrast to applications in computerized tomography, careful choice of the parametrisation of the problem and of the light path setup plays a major role. For a discrete approach using a linear parametrisation and a least squares minimum norm solution, we have shown that reconstruction errors in terms of overall quadratic deviations and errors for the total concentrations can be reduced by choosing the optimal dimension of the discretisation grid. Averaging over several reconstruction grids reduces accidental features. Analysis of an indoor experiment has shown that the impact of pure DOAS measurement errors on the reconstruction is moderate for the cases considered here. We have not studied other reconstruction principles, but work related to this topic is in progress.

Giving the reconstruction result in the form $c(\mathbf{r})\pm\Delta c(\mathbf{r})$, i.e. with an estimation of the reconstruction error field, as done by Laepple et al. (2004), is only possible with specific assumptions on the unknown distribution. In the same way, the effect of time dependent distributions is related to specific atmospheric conditions and the details of the measurement cycle. These questioned are currently addressed in the analysis of a tomographic experiment over the city center of Heidelberg (Pöhler et al., this issue) where three telescopes and 16 light paths at least will be used to monitor an area of 3×4 km^2.

6. ACKNOWLEDGEMENTS

The German Ministry of Research and Education (BMBF) is gratefully acknowledged for the funding of this work through project 07 ATC-03 (Young researchers fellowship program for research groups, AFO 2000-C).

7. REFERENCES

Drescher, A. C., Gadgil, A. J., Price, P. N., and Nazaroff, W. W., Novel approach for tomographic reconstruction of gas concentration distributions and simulated annealing, Atmos. Environ., 30, 929–940, 1996.

Drescher, A. C., Park, D. Y., Yost, M. G., Gadgil, A. J., Levine, S. P., and Nazaroff, W. W., Stationary and time-dependent indoor tracer-gas concentration profiles measured by OP-FTIR remote sensing and SBFM-computed tomography, Atmos. Environ., 31, 727–740, 1997.

Fischer, M. L., Price, P. N., Thatcher, T. L., Schwalbe, C. A., Craig, M. J., Wood, E. E., Sextro, R. G., and Gadgil, A. J., Rapid measurements and mapping of tracer gas concentrations in a large indoor space, Atmos. Environ., 35, 2837–2844, 2001.

Laepple, T., Knab, V., Mettendorf, K.-U., and Pundt, I., Longpath DOAS tomography on a motorway exhaust gas plume: numerical studies and application to data from the BABII campaign, Atmos. Chem. Phys., 4, 1323-1342, 2004.

Platt, U., Air monitoring by Differential Optical Absorption Spectroscopy (DOAS), In: Air Monitoring by Spectroscopic Techniques, M. W. Sigrist, Ed., Chemical Analysis Series, Vol. 127, John Wiley & Sons, Inc., New York, 1994.

Price, P. N., Fischer, M. L., Gadgil, A. J., Sextro, R. G., An algorithm for real-time tomography of gas concentrations using prior information about spatial derivatives, Atmos. Environ., 35, 2827-2835, 2001.

Pundt, I., Mettendorf, K.-U., Laepple, T., Knab, V., Xie, P., Lösch, J., v. Friedeburg, C., Platt, U., and Wagner, T., Measurements of trace gas distributions by Long-path DOAS-tomography during the motorway campaign BAB II: experimental setup and results for NO_2, Atmos. Environ, 39, 967-975, 2005.

Samanta, A., and Todd, L. A., Mapping chemicals in air using an environmental CAT scanning system: evaluation of algorithms, Atmos. Environ., 34, 699-709, 2000.

Todd, L. and Ramachandran, G., Evaluation of algorithms for tomographic reconstruction of chemical concentrations in indoor air, Am. Ind. Hyg. Assoc. J., 55, 403–416, 1994.

Todd, L., and Bhattacharyya, R., Tomographic reconstruction of air pollutants: evaluation of measurement geometries, Appl. Opt., 36, 7678-7688, 1997.

Verkruysse ,W., and Todd, L. A., Improved method "grid translation" for mapping environmental pollutants using a two-dimensional CAT scanning system, Atmos. Environ., 38, 1801-1809, 2004.

Wolfe, D. C., and Byer, R.L., Model studies of laser absorption computed tomography for remote air pollution measurement, Appl. Opt., 21, 1165-1177, 1982.

Yost, M. G., Gadgil, A. J., Drescher, A. C., Zhou, Y., Simonds, M. A., Levine, S. P., Nazaroff, W., and Saisan, P., Imaging indoor tracer-gas concentrations with computed tomography: experimental results with a remote sensing FTIR system, Am. Ind. Hyg. Ass. J., 55, 395-402, 1994.